books@ocg.at

Stefan Scherer (ed.)

Computer Vision, Computer Graphics and Photogrammetry - a Common Viewpoint

25th Workshop of the
Austrian Association for Pattern Recognition
(ÖAGM/AAPR)

ISBN 3-85403-147-5 Österreichische Computer Gesellschaft

Oesterreichische
Computer
Gesellschaft
http://www.ocg.at

Detection of Flaws on Melamine Faced Chipboards using Wavelet based Texture Analysis

Regine Bolter, Gustavo J. Fernandez, Gunther Lenz and Franz Leberl
Computer Graphics and Vision
Graz University of Technology
bolter@icg.tu-graz.ac.at, http://www.icg.tu-graz.ac.at

Abstract:
In this paper we present a wavelet based approach for the inspection of local defects embedded in homogeneous textured surfaces of melamine faced chipboards. The detection of defects within the inspected texture is performed by first partitioning the image into slightly overlapping tiles of size 2^n, decomposing these graylevel tiles into sub-bands using the discrete wavelet transform, calculating the energy value of the wavelet coefficients within each wavelet sub-band and finally classifying each tile as defective of non-defective with a Bayes classifier being trained on defect free samples a priori. The experimental results on 127 probes demonstrate the usefulness of this approach for the visual inspection of slightly textured melamine faced chipboards. 93.3% of the errors in the test samples are identified and only 0.06% false positives occur.

1 Introduction

An approach is needed for the detection of faint flaws on melamine faced chipboards in real time. Although this seems to be an easily solvable, local 2D task, special problems arise due to the boundary conditions. First of all the surfaces under inspection are bright but slightly textured with an irregular pattern. Second, a variety of errors can occur, ranging from small scale, dark dots to medium scale inclusions and bumps, up to linear dark and bright scratches and faults. Some bumps and scratches are even invisible expect when viewed from distinct, shallow directions. In the project specification, small scale denotes errors in the range of 0.08 mm^2 on areas of 360000 mm^2, and real time means 1000 pieces per hour which results in a processing time of 3,6 seconds per piece.

Automatic visual inspection techniques for textured surfaces generally compute a set of textural features in a sliding window, and search for significant local deviations in the feature values. A wide range of texture analysis methods has been proposed in the past. For re-

views, see e.g. [5] or [7]. The use of wavelets for texture analysis was pioneered by Mallat [4]. Chang and Kuo [1] proposed a tree-structured wavelet transform for texture classification. A set of textural features is derived from the energy values of dominant channels, and distance measures are then employed to discriminate textures. Laine and Fan [2] used both energy and entropy metrics of each decomposed wavelet packet as textural features. The number of features therefore is numerous, a two layer neural network uses those features as input for texture classification.

In this paper we first present our prototype image acquisition system and discuss the occurrence of some flaws in these images. Then we present the wavelet based texture analysis approach, and show first results.

2 Test Data

To create a well defined imaging situation which delivers reproducible test material under different illumination conditions, we set up a laboratory prototype (Figure 1). Plate probes of size 100 x 100 mm^2 can be inserted at position (1). Above the probe three different light sources are installed which can be switched independently from a PC connected via a serial port. A diffuse illumination unit with white LEDs is located at position (2), two directed light sources illuminating the probe from a shallow angle are positioned at the back (3) and on the left side (4). The reason for these two directed shallow light sources lies in the properties of the errors to detect, especially scratches and bumps which alter the topography of the probe can only be visualized under shallow illumination. Problems occur, if a scratch follows the direction of the light source and is therefore still invisible. To avoid such situations, a second light source is mounted at a 90 degree position to the first one. In the center above the probe, a Sony XCD-XS900 CCD camera with 1280x960 pixel resolution is mounted (5).

Images of probes showing typical errors under diffuse and directed illumination captured with the laboratory setup are shown in Figure 2. The top row shows subsections of the probes illuminated by diffuse light, the corresponding subsections under directed light from one of the two light sources are shown in the bottom row. From left to right the first image (a) is a typical example of dust spots, some of these dust spots are just a few pixels wide and usually invisible in shallow directed illumination (e). The third pair (c) and (g) show a typical inclusion, which is visible in both illuminations. On the other hand the scratch in the second probe (b),(f) is only visible in the directed illumination (f), the same is true for the slight bump in (d) and (h) of the same figure.

Altogether 127 single sided probes of the size 100 x 100 mm^2 with various errors of the kind just presented are available for our study. The first experiments were performed with three different illuminations, one image under diffuse illumination and two images using directed

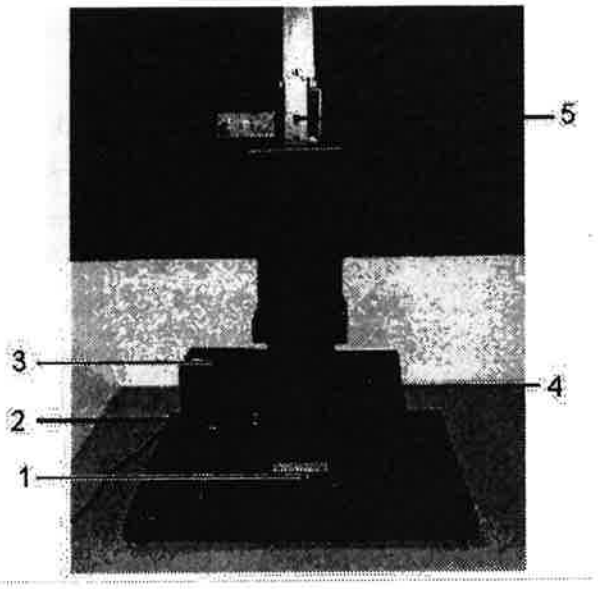

Figure 1: Laboratory prototype for image acquisition

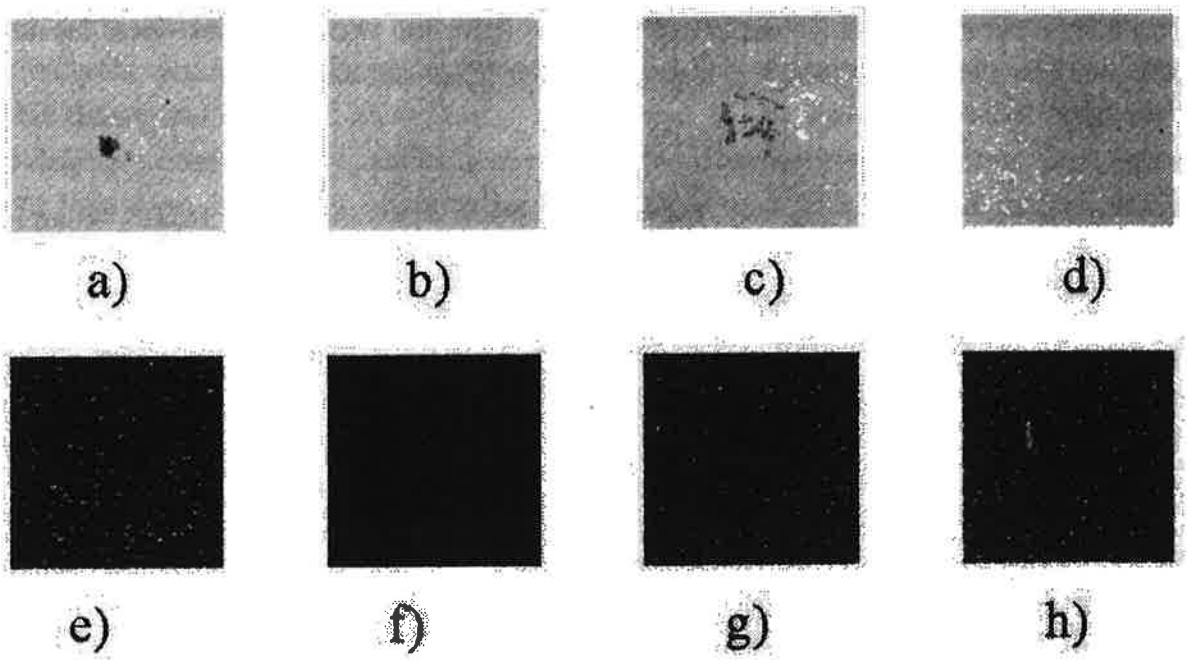

Figure 2: Probes showing typical errors, imaged using diffuse (top row) and directed (bottom row) illumination.

illumination either from the back and or from the left of the probe. However, because of our tight time budget we reduced the testset to two images per probe, one under diffuse illumination and a second one with both directed light sources switched on for a single image.

3 Methods

Our first approach was to apply simple local and global thresholds to the images. Best results were achieved using local thresholds derived from statistical features of the graylevels on the images captured with diffuse illumination. However, not all errors could be identified by this method, especially linear features were detected only partially. The images captured under directed light were analyzed with different texture filters like Gabor filters and Laws texture filters, the results were comparable to the results obtained from threshold on the diffuse illuminated images, still some errors, especially linear features were detected just partially. The reason for this is that these texture filters are usually applied to classify different textures, whereas in our case we want to detect even small deviations from the given texture.

Compared to these results, texture analysis based on the discrete Wavelet transform (DWT) [4] delivered better results at first go. The whole images were subdivided into tiles of size 32x32 pixels. A DWT with three levels was performed on these tiles. Various statistical features, as e.g., energy, standard deviation, mean, maximum, were calculated on the subbands of the different levels and their usefulness for error detection was examined. Best results were achieved calculating the energy E over all levels n in the subbands i [3]:

$$E_{ni} = \frac{1}{N} \sum_{N} (D_{ni}(b_j, b_k))^2 \tag{1}$$

where b_j and b_k are the indices to the N discrete wavelet coefficients D_{ni} within the subband i and the level n. Using tiles of size 32x32 pixels, three wavelet decomposition levels with three subbands each were used, this results in 9 energy values per tile. These 9 energy values are then used to classify the 32x32 pixel tile using a Bayes classification scheme. As was already mentioned the smallest error which has to be detected has a size of $0.08mm^2$. To avoid problems along the border of the tiles we used an overlap of two pixels between adjacent tiles. Applying this scheme of image subdivision into overlapping tiles, wavelet decomposition and calculation of 9 energy values per tile for the classification result in a data reduction of 100:1 from the original image of the size 930x930 pixels to 31x31 overlapping tiles with 9 energy values per tile. This is an important factor considering the real time applicability of the approach.

The purpose of the classification system is to classify each tile of an image based on the 9 energy values into one of the two classes defective or non-defective. Where defective means in our case if an error larger in size than $0.08mm^2$ occurs. For the supervised Bayesian classification scheme training data is necessary. This was collected manually for a training set of 31 images by inspecting the tiles in detail. To ensure finding all errors larger than $0.08mm^2$ in the training set only perfect tiles where classified as non-defective. The Bayes discriminant

functions assuming normal distributions in the classes according to [6] are:

$$g_i(\vec{x}) = -\frac{1}{2}\vec{x}^T\Sigma_i^{-1}\vec{x} + \frac{1}{2}\vec{x}^T\Sigma_i^{-1}\mu_i - \frac{1}{2}\mu_i^T\Sigma_i^{-1}\mu_i + \frac{1}{2}\mu_i^T\Sigma_i^{-1}\vec{x} + \ln P(\omega_i) - \frac{l}{2}\ln 2\pi - \frac{1}{2}\ln|\Sigma_i| \quad (2)$$

where $\vec{x}$ is the sample vector to classify, Σ_i is the covariance matrix of class i, μ_i is the mean value of class i, and $P(\omega_i)$ is the a priori probability of class ω_i. For each sample vector $\vec{x}$ Equation 2 is evaluated for both classes and the tile is classified according to the maximum.

4 Results

The results of the error detection based on the Bayes classification of the 9 energy values within the wavelet subbands were evaluated on a training set of 31 images and on a testset of 94 images. Each image consists of 31x31 tiles, where each tile is a separate sample for the training and classification, this results in 29.791 samples for training and 90.334 different samples for testing the system. The groundtruth was obtained from visual classification using two different assumptions for training and testing. In the training samples, each tile with a visible defect was classified as defective, independent of the size of the defect, because the non-defective class should consist only of perfect tiles. However, for the test data only defects larger than 8 pixels, corresponding to area error larger than $0.08mm^2$ were marked, because only these errors have to be detected. Due to the large amount of training and test data and the different groundtruth assumptions, we do not use a cross validation for the evaluation of the classifier. The classification results for the training and testset are given in Table 1.

	Samples	Errors	Correct	False Negatives	False Positives
Training Set	29791	520	332	188	62
		100%	63.8%	36.1%	
Test Set	90334	1431	1335	96	513
		100%	93.3%	6.7%	

Table 1: Bayes classification results for the wavelet based texture analysis on the training set and test set. The percentage values for correct and false negative detected errors refer to the total number of errors occurring, denoted as 100% in the table.

One might be surprised that the results on the training set are worse compared to the results on the testset. The reason for this fact lies in the different assumptions for the groundtruth data. If one considers only errors larger than $0.08mm^2$ the performance on the training set increases to 98.2%. The number of false positives seems to be quite high, especially for the test set. However, compared to the whole class of good tiles, only 0.2% were misclassified for

the training set and only 0.6% of the testset. Visual inspection of these false positives revealed only 7 real false positives, where no defect is visible in the training set and only 50 real false positives for the test set, which is a reduction to 0.02% for the training set and 0.06% for the testset.

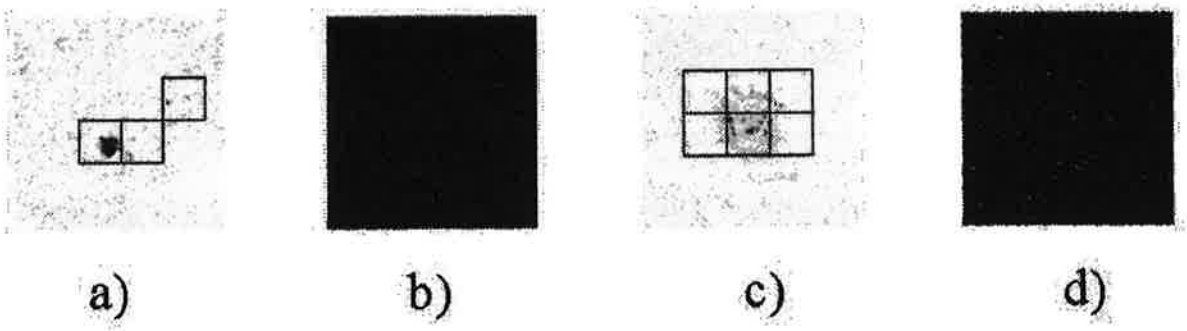

Figure 3: Wavelet based error detection applied to the samples shown in Figure 2.

Some results of the wavelet based error detection can be seen from Figure 3. The Bayes classification works quite well on the errors visible under diffuse illumination, dust and inclusions can be identified by the method, as can be seen from Figure 3 (a) and (c). The scratch in Figure 2 (b) and (f) could be identified by the same classification method by first calculating the gradient on the image captured with directed illumination and applying the wavelet analysis to the gradient image. The same procedure worked for the bump in Figure 2 (h), which was identified in Figure 3 (d).

5 Discussion and Outlook

These first results are very promising, the method is applicable to the slightly textured probes, almost all visible flaws could be detected. Visual inspection revealed that most of the false negatives are tiles at the border of larger area errors, where the main error was detected. There are still quite a few false positives, incorporation of a rejection class might help to overcome this problem. Using only the energy of the DWT coefficients, an exact border between errors smaller than $0.08mm^2$ and larger than $0.08mm^2$ can not be drawn, this can be seen from the number of false positives. From the 513 false positives in the testset only 50 show really no defect, in all other cases a small but high contrast defect is present. Maybe the inclusion of further features, especially the minimum, maximum and mean grayvalues of the tiles can help to overcome these problems.

We also did some experiments on our training data using Gabor filters and Laws texture filters, the results of the wavelet based texture analysis clearly outperform these classical texture

analysis methods considering classification performance and processing time. Especially Gabor filters are extremely time consuming. The DWT based texture analysis method seems to be fast enough for a real time application, the processing time for an image of the size 930 x 930 pixels is below two seconds without any code optimization. If necessary, the algorithms for gradient calculation on the direct illuminated images and the wavelet decomposition could be executed on a fast signal processor, therefore the real time application of the presented method to the original problem seams feasible.

Acknowledgment

The authors wish to thank Johann Kandlbauer for providing the wavelet decomposition and energy calculation software.

References

[1] Tianhorng. Chang and C.-C. Jay Kuo. Texture analysis and classification with tree-structured wavelet transform. *IEEE Transactions on Image Processing*, 2(4):429–441, 1993.

[2] Andrew Laine and Jian Fan. Texture classification by wavelet packet signatures. *IEEE Transactions on Pattern Analysis and Machine Intelligence*, 15(11):1186–1191, 1993.

[3] Livens, S. and Scheunders, P. and Van de Wouwer, G. and Van Dyck, D. Wavelets for Texture Analysis, an Overview. In *6th Int. Conf. on Image Processing and its Applications*, volume 2, pages 581–585, Dublin, Ireland, July 1997.

[4] Stephane G. Mallat. A theory for multiresolution signal decomposition: the wavelet representation. *IEEE Trans. PAMI*, 11(7):674–693, 1989.

[5] Timothy S. Newan and Anil K. Jain. A survey of automated visual inspection. *Computer Vision and Image Understanding*, 61(2):231–262, 1995.

[6] Sergios Theodoridis and Konstantinos Koutroumbas. *Pattern Recognition*. Academic Press, 1998.

[7] Du-Ming Tsai and Bo Hsiao. Automatic surface inspection using wavelet reconstruction. *Pattern Recognition*, 34:1285–1305, 2001.